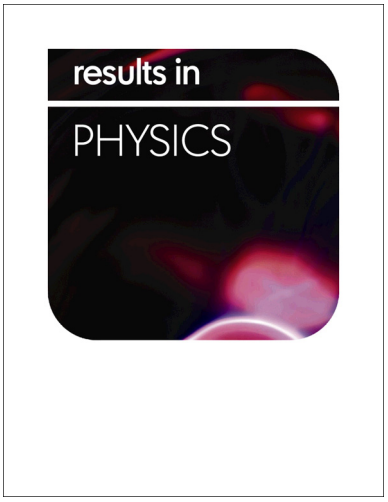

MHD Pulsatile Flow of Engine oil based Carbon Nanotubes between Two Concentric Cylinders

Rizwan Ul Haq, Faisal Shahzad, Qasem M. Al-Mdallal

PII: S2211-3797(16)30327-8
DOI: http://dx.doi.org/10.1016/j.rinp.2016.11.057
Reference: RINP 457

To appear in: *Results in Physics*

Received Date: 7 October 2016
Revised Date: 23 November 2016
Accepted Date: 25 November 2016

Please cite this article as: Ul Haq, R., Shahzad, F., Al-Mdallal, Q.M., MHD Pulsatile Flow of Engine oil based Carbon Nanotubes between Two Concentric Cylinders, *Results in Physics* (2016), doi: http://dx.doi.org/10.1016/j.rinp.2016.11.057

MHD Pulsatile Flow of Engine oil based Carbon Nanotubes between Two Concentric Cylinders

Rizwan Ul Haq[1,*], *Faisal Shahzad* [2]

[1]*Department of Electrical Engineering, Bahria University, Islamabad Campus, Islamabad, 44000, Pakistan*

[2]*Department of Mathematics, Capital University of Science and Technology, Islamabad 44000, Pakistan*

Abstract

Present analysis is dedicated to examine the thermal performance of engine oil in the presence of both single and multiple wall carbon nanotubes (SWCNTs and MWCNTs) between two concentric cylinders. Flow is driven with oscillatory pressure gradient and magneto-hydrodynamics (MHD) effects are also introduced to control the random motion of the nanoparticles. Arrived broad, it is perceived that the inclusion of nanoparticles increases the thermal conductivity of working fluid significantly for both turbulent and laminar regimes. Fundamental momentum and energy equations are based upon partial differential equations (PDEs) that contain thermos-physical properties of both SWCNTs and MWCNTs. The solution has been evaluated for each mixture, namely: SWCNT-engine oil and MWCNT-engine oil and results are determined for each velocity, temperature, pressure and stress gradient. Graphical results for the numerical values of the emerging parameters, namely: Hartmann number M, the solid volume fraction ϕ of the nanoparticles, Reynolds number Re_{ω}, and the pulsation parameter based on the periodic pressure gradient are analyzed for pressure difference, frictional forces, velocity profile, temperature profile and vorticity phenomena. The assets of various parameters on the flow quantities of observation are investigated. To the same degree a concluding crux, the streamlines are examined and plotted for engine oil based CNTs. Womersley number and nanoparticle volume fraction demonstrate the significant effects on nanofluid flow with in the restricted domain of ducts due to dependence of dynamic viscosity. Based upon whole analysis it concludes that engine oil based SWCNTs provides higher velocity and temperature profile as compared to the engine oil based MWCNTs.

Keywords: MHD, Pulsating flow, nanofluids, carbon nanotubes, concentric cylinders.

[*] Contact: *ideal_riz@hotmail.com* , *r.haq.qau@gmail.com* (R. U. Haq)
+92 333 5371853

1. Introduction

The study of pulsatile flow has attained considerable attention based on several investigations at industrial level. Flows in a conduit/cylinder brought about via sinusoidal influence in the waves transmitting alongside of the channel's walls are determined through pulsatile flows. The study of the fluids that reveal oscillatory flow have numerous important application in nature, common examples in medical sciences included; blood flow through an artery, peristaltic food motion in the intestine and motion of urine in the urethra. In astrophysics and geophysics, its miles implemented to the have a look at of stellar shape, cores terrestrial and sun plasma.

In the early stages, H. B. Atabek et al. [1] calculated the time dependent flow in tubular pipe and carried out the analytical results for variation of the velocity profile. After this concept, Vardanyan et al. [2] have developed several theoretical models on the influence of magnetic strength of pulsatile type flow. They have mentioned that the presence of the consistent and uniform magnetic strength decreases the flow rate; their work has a significant impact on biological research. Richardson and Tyler [3, 4] presented the experimental results in the existence of one of the important structures of oscillating flow that is named as annular effect. Subsequent studies of Womorsley [5] and Uchida [6] established these results by analyzing the sinusoidal motion of the incompressible fluid oscillating along a flat conduit. Apart from all above theoretical study, the real world applications related to the present analysis are deal for various physical geometries are mentioned by various authors. Recently, Yang et al. [7] presented the idea of optimization for whole cylinder with pin-fin heat sink with the finite volume method and maximum heat transfer rate is utilized to maintain the pressure drop, fin-material volume and heat sink volume. In another study Cui et al. [8] described the parametric illustration to estimate the thermal performance of a counter-flow reformative indirect evaporative heat exchange and it is found that this phenomena is able to predict the performance of the counter-flow regenerative IEHX within inconsistency of 12%. Similarly to impact of hydrogen and producer gasses as ordinary fuels on combustion constraints of a dual fuel diesel machine is proposed by Dhole et al. [9] and it is concluded that the heat discharge rate in the first phase of combustion found to decrease during both types of fuel substitution as compared to diesel fuel. There are vast articles presented by various authors to deal the heat transfer phenomena [10-12].

Dulal Chandra Sanyal and Ananda Biswas [13] have proven under the normal conditions, blood goes with the flow inside the human's cardiovascular structure relies the pumping action of the heart and this system produces a pressure gradient throughout the arteries. Yakhot et al. [14] examined the effect of pressure gradient rate in the velocity with phase difference along the axial velocity. These phases are differences fluctuate which start from 0 degrees to the small frequencies up to 90 degrees from the highest level of frequencies. Suces et al. [15] numerically examined the reaction features of the wall temperature and the average temperature between laminar fluid drift and a horizontal flat plate by mean of finite difference technique (FDM). Latham [16] was the first person who discussed the peristaltic flow. Later on, researchers and scientists emphasized their considerations to analyses the peristaltic flows with different fluid models and geometries. Majdalani [17] resolved the precise solution of limiting case of the Navier-Stokes equation that governs the pulsatile glide through a cylindrical pipe where the stress gradient is changed by using the Fourier coefficients. Agrawal et al. [18] present a mathematical model that deals with the impact of magnetic strength of the blood flow via similarly branched channel with different partitions. During this observation they have observed that magnetic strength may be used as a blood pump of wearing out cardiac processes to treatment few arteries diseases. E.E. Tzirtzilakis [19] discussed a mathematical model for bio magnetic fluid dynamics (BFD), appropriate for the description of the Newtonian blood float beneath the motion of magnetic field. G. Ramamurthy et al. [20] studied the magneto-hydrodynamic (MHD) results in blood flow via a porous channel.

In the recent development of science and technology, study of nanofluid attained considerable attention due to its wide applications. Nanofluid is just a fluid comprising nanometer-sized particles, referred to as nanoparticles. One of the most important features of nanofluid is to enhance the heat transfer by improving the thermal conductivity of working fluids. This invention was first conceived by Choi [21]. Nanofluids require some important thermos-physical properties of both particle and fluid such as: thermal diffusivity, viscosity, thermal conductivity, and convective heat transfer coefficients comparable [22-25]. Buongiorno [26] presented after effect of heat alteration on the carriage of nanofluid via important slip mechanism. Akbar et al. [27] discussed the mixed convection flow of Jeffrey nanofluid with magnetic field effects. Ebaid et al. [28] discussed about nanofluids within the boundary layer

region and exact solution acquired from the governing equation with distinct values of emerging physical parameters.

The CNTs are one of the most important and significant material in the form of tubular cylinder of carbon atoms having astonishing mechanical, electrical and thermal performance. The CNTs can appearance high achievement because of their amazing electronic, mechanical, and structural backdrop such as baby admeasurement and mass, stronger, higher electrical and thermal conductivity, and so forth [29]. The carbon atoms that anatomy nanotubes are abiding in a hexagonal network 1 nm in bore and one hundred m in length can about be anticipation of as a band of graphite formed up into a cylinder [30]. There are three types of CNTs i.e. single, double and multiple wall carbon nanotubes, which alter in the adjustment of their graphene cylinders. According to latest research, Elena et al. [31], only saturation of nanoparticles are not enough to enhance the heat transfer. They have discussed the thermal conductivity of various shapes of particle and it is determine that plats shape particle provides best and higher thermal conductivity as compare to the other of shapes of the particles. In agreement with Murshed et al. [32], it is found that CNTs have approximately six times superior thermal conductivity as compare to the other base fluids and materials at room temperature. Mainly the benefits of CNT include additives in polymers, lithium-battery anodes, nanolithography, super capacitor, hydrogen storage, electromagnetic-wave absorption and shielding gas-discharge tubes in telecom networks. Apart from these CNTs can be used for quantum dots, drug delivery, drug discovery, implantable Nano sensors and Nano robots, actuators and Nano fluidic system.

In the view of above literature survey, main objective of the present framework is to analyze the heat transfer of engine oil based CNTs between two concentric cylinders. Two kinds of nanoparticles namely SWCNTs and MWCNTs are analyzed within the base fluid. Flow is generated due to oscillatory pressure gradient. The governing equations of described model are then solved analytically to achieve the precise answers of Bessel function of first and second kind. The obtained expressions for velocity, temperature and pressure gradient are discussed graphically through variant in bodily parameters. Dominant difference can be found in the velocity and temperature profile for each mixture: engine oil-SWCNTs and engine oil-MWCNTs. Pressure gradient is also calculated for different values of time.

Nomenclature

C	specific heat
k	thermal conductivity
M	Hartmann number
R	radius of cylinder
Pr	Prandtl number
Re_ω	Reynolds number
I_0	Bessel functions of first kind
K_0	Bessel functions second kind
t	time
D	diameter
r	radius
T	temperature
u, v, w	Velocity components
$\vec{J}$	Current density
$\vec{B}$	Magnetic field
H	Magnetic field intensity
L	Length of the cylinder
P	Pressure
A	Amplitude
CNT	Carbon nanotube
SWCNT	single wall carbon nanotubes
MWCNT	Multiple wall carbon nanotubes
Greek symbols	
ρ	density
μ	dynamic viscosity
ν	kinematic viscosity
σ	electric conductivity
α	Womersley Number ($= \sqrt{Re_\omega}$)
γ	temperature gradient
ϕ	volume fraction of the nanoparticles
ω	pulsation
Subscripts	
i	internal
e	external
f	base fluid
p	particle
nf	Nanofluid
f	base fluid

2. Mathematical formulation

2.1 Physical problem

An electrically conducting viscous, incompressible fluid is flowing between two concentric cylinders as shown in Fig.1. Fluid is moving within the concentric cylinder due to pulsatile pressure gradient and constant magnetic field that is applied in the direction of z-axis. In the beginning, the inner cylinder is at a temperature of 400 *Kelvin* and the outer cylinder has adiabatic condition with atmospheric pressure and a temperature of 300 *Kelvin*.

2.2 Governing equations

We have considered incompressible, viscous and electrically conducting fluid, the flow is laminar and symmetric in both directions. By neglecting the energy losses because of law of conservation of mass and the constant magnetic field is acting in the radial direction. The conventional continuity, momentum and energy equations are:

$$\nabla.\vec{V} = 0 \tag{1}$$

$$\rho_{nf}\left(\frac{\partial\vec{V}}{\partial t} + \vec{V}\cdot\nabla\vec{V}\right) = -\nabla P + \mu_{nf}\nabla^2\vec{V} + \left(\vec{J}\times\vec{B}\right)\vec{V}, \tag{2}$$

$$(\rho C)_{nf}\left(\frac{\partial T_f}{\partial t}+\left(\vec{V}\cdot\nabla T_f\right)\right)=k_{nf}\nabla^2 T. \tag{3}$$

In cylindrical coordinates system, equation of continuity, momentum and energy are given to be:

$$\frac{\partial u}{\partial r}+\frac{\partial w}{\partial z}+\frac{u}{r}=0, \tag{4}$$

$$\rho_{nf}\left(\frac{\partial u}{\partial t}+u\frac{\partial u}{\partial r}+w\frac{\partial u}{\partial z}\right)=-\frac{\partial P}{\partial r}+\mu_{nf}\left[\frac{\partial^2 u}{\partial r^2}+\frac{1}{r}\frac{\partial u}{\partial r}+\frac{\partial^2 u}{\partial z^2}-\frac{u}{r^2}\right], \tag{5}$$

$$\rho_{nf}\left(\frac{\partial w}{\partial t}+u\frac{\partial w}{\partial r}+w\frac{\partial w}{\partial z}\right)=-\frac{\partial P}{\partial z}+\mu_{nf}\left[\frac{\partial^2 w}{\partial r^2}+\frac{1}{r}\frac{\partial w}{\partial r}+\frac{\partial^2 w}{\partial z^2}\right]-\sigma_{nf}B_o^2 w, \tag{6}$$

$$(\rho C)_{nf}\left(\frac{\partial T}{\partial t}+u\frac{\partial T}{\partial r}+w\frac{\partial T}{\partial z}\right)=k_{nf}\left[\frac{\partial^2 T}{\partial r^2}+\frac{1}{r}\frac{\partial T}{\partial r}+\frac{\partial^2 T}{\partial z^2}\right]. \tag{7}$$

In the above equations u and w are velocities along r and z direction, respectively. Similarly P and T are the pressure and temperature. Where: ρ_{nf}, μ_{nf}, $(\rho C)_{nf}$, k_{nf} and σ_{nf} is density, viscosity, specific heat, thermal and electric conductivity of nanofluid respectively. Also

$$\rho_{nf}=(1-\phi)\rho_f+\phi\rho_{CNT}, \tag{8a}$$

$$(\rho C)_{nf}=(1-\phi)(\rho C)_f+\phi(\rho C)_{CNT}, \tag{8b}$$

$$\frac{k_{nf}}{k_f}=\frac{1-\phi+2\phi\left(\frac{k_{CNT}}{k_{CNT}-k_f}\right)ln\left(\frac{k_{CNT}+k_f}{2k_f}\right)}{1-\phi+2\phi\left(\frac{k_f}{k_{CNT}-k_f}\right)ln\left(\frac{k_{CNT}+k_f}{2k_f}\right)}, \tag{8c}$$

$$\mu_{nf}=\frac{\mu_f}{(1-\phi)^{2.5}}. \tag{8d}$$

In the above expressions ρ_f, C_f, k_f, μ_f is the density, specific heat, thermal conductivity, dynamic viscosity of working fluid, respectively. Similarly ρ_{CNT}, C_{CNT}, k_{CNT} is the density, specific heat, thermal conductivity of the fluid, thermal conductivity of the CNT respectively. Where, ϕ is nanoparticle volume fraction. In view of above mentioned quantities, the conservation law of momentum and energy are reduced to

$$\left((1-\phi)\rho_f+\phi\rho_{CNT}\right)\left(\frac{\partial u}{\partial t}+u\frac{\partial u}{\partial r}+w\frac{\partial u}{\partial z}\right)=-\frac{\partial P}{\partial r}+\left(\frac{\mu_f}{(1-\phi)^{2.5}}\right)\left[\frac{\partial^2 u}{\partial r^2}+\frac{1}{r}\frac{\partial u}{\partial r}+\frac{\partial^2 u}{\partial z^2}-\frac{u}{r^2}\right] \tag{9a}$$

$$\left((1-\phi)\rho_f + \phi\rho_{CNT}\right)\left(\frac{\partial w}{\partial t} + u\frac{\partial w}{\partial r} + w\frac{\partial w}{\partial z}\right) = -\frac{\partial P}{\partial z} + \frac{\mu_f}{(1-\phi)^{2.5}}\left[\frac{\partial^2 w}{\partial r^2} + \frac{1}{r}\frac{\partial w}{\partial r} + \frac{\partial^2 w}{\partial z^2}\right] - \sigma_f B_o^2 w \quad (9b)$$

$$\left((1-\phi)(\rho C)_f + \phi(\rho C)_{CNT}\right)\left(\frac{\partial T}{\partial t} + u\frac{\partial T}{\partial r} + w\frac{\partial T}{\partial z}\right) = k_{nf}\left[\frac{\partial^2 T}{\partial r^2} + \frac{1}{r}\frac{\partial T}{\partial r} + \frac{\partial^2 T}{\partial z^2}\right] \quad (9c)$$

The system can be expressed in dimensionless terms by defining the following quantities;

$u = \frac{u'}{\omega R_e}, w = \frac{w'}{\omega R_e},\ r = \frac{\acute{r}}{R_e}, z = \frac{\acute{z}}{R_e},\ t = \omega t', T = \frac{T\prime - T_f}{T_i - T_f}, P = \frac{P\prime}{\rho_f R_e^2 \omega^2}, \nu_f = \frac{\mu_f}{\rho_f}, Re_\omega = \alpha^2 = \frac{\omega R_e^2}{\nu_f}, Pr = \frac{\mu_f C_f}{k_f}, M = R_e B_o \sqrt{\frac{\sigma_f}{\mu_f}}$.

In the above expression Re_ω is the Reynolds number, Pr is the Prandtl number and M is the Hartmann number. Dimensionless form of the equations 9(a)-9(c) takes the following form;

$$A_1\left(\frac{\partial u}{\partial t} + u\frac{\partial u}{\partial r} + w\frac{\partial u}{\partial z}\right) = -\frac{\partial P}{\partial r} + \frac{1}{(1-\phi)^{2.5} Re_\omega}\left[\frac{\partial^2 u}{\partial r^2} + \frac{1}{r}\frac{\partial u}{\partial r} + \frac{\partial^2 u}{\partial z^2} - \frac{u}{r^2}\right], \quad (10a)$$

$$A_1\left(\frac{\partial w}{\partial t} + u\frac{\partial w}{\partial r} + w\frac{\partial w}{\partial z}\right) = -\frac{\partial P}{\partial z} + \frac{1}{(1-\phi)^{2.5} Re_\omega}\left[\frac{\partial^2 w}{\partial r^2} + \frac{1}{r}\frac{\partial w}{\partial r} + \frac{\partial^2 w}{\partial z^2}\right] - \frac{M^2 w}{Re_\omega}, \quad (10b)$$

$$A_2\left(\frac{\partial T}{\partial t} + u\frac{\partial T}{\partial r} + w\frac{\partial T}{\partial z}\right) = \frac{A_3}{Pr Re_\omega}\left[\frac{\partial^2 T}{\partial r^2} + \frac{1}{r}\frac{\partial T}{\partial r} + \frac{\partial^2 T}{\partial z^2}\right]. \quad (10c)$$

Where, the coefficients A_1, A_2 and A_3 are defined as:

$$A_1 = (1-\phi) + \phi\frac{\rho_{CNT}}{\rho_f}, \quad (11a)$$

$$A_2 = (1-\phi) + \phi\frac{(\rho C)_{CNT}}{(\rho C)_f}, \quad (11b)$$

$$A_3 = \frac{k_{nf}}{k_f} = \frac{1-\phi+2\phi\left(\frac{k_{CNT}}{k_{CNT}-k_f}\right)ln\left(\frac{k_{CNT}+k_f}{2k_f}\right)}{1-\phi+2\phi\left(\frac{k_f}{k_{CNT}-k_f}\right)ln\left(\frac{k_{CNT}+k_f}{2k_f}\right)}. \quad (11c)$$

2.3 Boundary Conditions

The associated initial and boundary conditions of the model will take the following form;

At $t = 0$

$$u(r,z,0) = w(r,z,0) = 0 \quad \text{and} \quad p(r,z,0) = T_f(r,z,0) = 0, \quad (12a)$$

For external duct:

$$u(1,z,t) = w(1,z,t) = 0 \quad \text{and} \quad \frac{\partial T_f}{\partial r}(1,z,t) = 0 \tag{12b}$$

For internal duct:

$$u\left(\frac{R_i}{R_e},z,t\right) = w\left(\frac{R_i}{R_e},z,t\right) = 0 \quad \text{and} \quad T_f\left(\frac{R_i}{R_e},z,t\right) = 1 \tag{12c}$$

To find the analytical solution of given model, we have assumed that flow is fully developed and velocity field is defined as:

$$\vec{V} = [0,0,w(r,z,t)]. \tag{13}$$

The simplified form of governing equations can be rewrite in the following form,

$$A_1 \frac{\partial w}{\partial t} = -\frac{\partial p}{\partial z} - \frac{1}{(1-\phi)^{2.5}\mathrm{Re}_\omega}\left[\frac{\partial^2 w}{\partial r^2} + \frac{1}{r}\frac{\partial w}{\partial r}\right] - \frac{M^2}{\mathrm{Re}_\omega} w, \tag{14a}$$

$$A_2\left(\frac{\partial T}{\partial t} + w\frac{\partial T}{\partial z}\right) = \frac{A_3}{Pr Re_\omega}\left[\frac{\partial^2 T}{\partial r^2} + \frac{1}{r}\frac{\partial T}{\partial r} + \frac{\partial^2 T}{\partial z^2}\right]. \tag{14b}$$

As flow problem is axis-symmetry, this analysis could be reduced within the annular space between two concentric cylinders. The dimensionless form of equation (14a) and (14b) becomes:

$$A_1 \frac{\partial w}{\partial t} = -\frac{\partial p}{\partial z} - \frac{A_4}{\alpha^2}\left[\frac{\partial^2 w}{\partial r^2} + \frac{1}{r}\frac{\partial w}{\partial r}\right] - \frac{M^2}{\alpha^2} w, \tag{15a}$$

$$A_2\left(\frac{\partial T}{\partial t} + w\frac{\partial T}{\partial z}\right) = \frac{A_3}{Pr\alpha^2}\left[\frac{\partial^2 T}{\partial r^2} + \frac{1}{r}\frac{\partial T}{\partial r} + \frac{\partial^2 T}{\partial z^2}\right], \tag{15b}$$

Where $A_4 = \frac{1}{(1-\phi)^{2.5}}$.

2.4 Solution of the problem

Since the present phenomena deals the study of pulsatile flow, therefore pressure gradient could be expressed in the form,

$$\frac{\partial P}{\partial z} = -\bar{A}.Cos(\omega.t) = Real(-\bar{A}e^{i\omega t}). \tag{16}$$

The suppose form solution for velocity profile can be defined as

$$w(r,t) = Real\left(f(r)e^{i\omega t}\right) \tag{17}$$

In view of above equations, we have from equation (15a)

$$\frac{d^2f(r)}{dr^2}+\frac{1}{r}\frac{df(r)}{dr}-\frac{1}{A_4}(M^2+i\alpha^2A_1)f(r)=-\frac{1}{A_4}\bar{A}\alpha^2 \tag{18}$$

The solution obtained from equation (18) is in the shape of Bessel function, that is:

$$f(r)=C_1I_0(\zeta r)+C_2K_0(\zeta r), \tag{19}$$

Where I_0 Bessel functions of first kind and K_0 are Bessel functions second kind. Where $\zeta=\sqrt{M^2+i\alpha^2A_1}$. To determine C_1 and C_2, we will use the boundary conditions

$$r=\frac{R_i}{R_e}=R_i^*, r=1 \quad w=0, \tag{20}$$

From equation (17) velocity solution profile can be indicted as

$$w(r,t)=Real\left[C_1I_0(\zeta r)+C_2K_0(\zeta r)+\frac{\bar{A}\alpha^2}{A_4\zeta^2}\right]e^{it}, \tag{21}$$

Where $C_1=-\frac{\alpha^2BesselK[0,\zeta]\bar{A}-\alpha^2BesselK[0,\zeta R^*]\bar{A}}{\zeta^2(BesselI[0,\zeta R^*]BesselK[0,\zeta]-BesselI[0,\zeta]BesselK[0,\zeta R^*])A_4}$ and

$$C_2=-\frac{-\alpha^2BesselI[0,\zeta]\bar{A}+\alpha^2BesselI[0,\zeta R^*]\bar{A}}{\zeta^2(BesselI[0,\zeta R^*]BesselK[0,\zeta]-BesselI[0,\zeta]BesselK[0,\zeta R^*])A_4}.$$

To determine the analytical solution of Eq. (15b), we suppose that solution of temperature profile can be represented as:

$$T(r,z,t)=Real\left[-\gamma^*z+\gamma^*\,g(r)\,e^{it}+1\right], \tag{22}$$

Where $\gamma^*=\frac{Re}{L}$, from equation (15b) we have

$$\frac{d^2g(r)}{dr^2}+\frac{1}{r}\frac{dg(r)}{dr}-i\frac{A_2\alpha^2Pr}{A_3}g(r)=\frac{A_2\alpha^2Pr}{A_3}f(r), \tag{23}$$

Using the boundary conditions,

$$r=R_i^*\Longrightarrow T=1 \text{ and } r=1\Longrightarrow\frac{\partial T}{\partial r}=0. \tag{24}$$

We have supposed that solution of temperature profile can be indicated as:

$$T(r,z,t) = Real[-\gamma^* z + \gamma^*[-iC_1 I_0(\zeta r) - iC_2 K_0(\zeta r) + C_3 I_0(\xi r) + C_4 K_0(\xi r) - \frac{i\bar{A}\alpha^2}{\zeta^2}]e^{it} + 1]\Big\} \quad (25)$$

Where, $\xi = \alpha\sqrt{\frac{iPrA_2}{A_3}}$,

$$C_3 = \frac{\alpha\zeta^2\sqrt{\text{iPr}}\sqrt{A_2}A_4\text{BesselK}[1,\xi]\delta_1 + \zeta^3\sqrt{A_3}A_4\text{BesselK}[0,\xi R^*]\delta_2}{\alpha\zeta^2\sqrt{\text{iPr}}(\text{BesselI}[1,\xi]\text{BesselK}[0,\xi R^*] + \text{BesselI}[0,\xi R^*]\text{BesselK}[1,\xi])},$$

$$C_4 = \frac{\alpha\zeta^2\sqrt{\text{iPr}}\sqrt{A_2}A_4\text{BesselI}[1,\xi]\delta_1 - \zeta\sqrt{A_3}A_4\text{BesselI}[0,\xi R^*]\delta_2}{\alpha\zeta^2\sqrt{\text{iPr}}(\text{BesselI}[1,\xi]\text{BesselK}[0,\xi R^*] + \text{BesselI}[0,\xi R^*]\text{BesselK}[1,\xi])},$$

$$\delta_1 = i\left[\text{BesselI}[0,\zeta R^*]C_1 + \text{BesselK}[0,\zeta R^*]C_2 + \frac{\alpha^2}{A_4\zeta^2}\bar{A} - i\frac{z}{e^{\text{it}}}\right],$$

$$\delta_2 = i[\text{BesselI}[1,\zeta]C_1 - \text{BesselK}[1,\zeta]C_2].$$

2.5 Pressure calculation

From equation (15a) we have

$$\frac{\partial P}{\partial z} = -\bar{A}_1\frac{\partial w}{\partial t} + \frac{A_4}{\alpha^2}\left[\frac{\partial^2 w}{\partial r^2} + \frac{1}{r}\frac{\partial w}{\partial r}\right] - \frac{M^2 w}{\alpha^2}. \quad (26)$$

Substituting the solution obtained for $w(r,t)$ in equation (26)

$$\frac{\partial P}{\partial z} =$$

$$-A_1\left(ie^{it}\left(\frac{\text{BesselI}[0,r\zeta]c_1}{\zeta^2 A_4^2} - \frac{\text{BesselK}[0,r\zeta]c_2}{\zeta^2 A_4^2} + \frac{\alpha^2 * \bar{A}}{({A_4}^2 * \zeta^2)}\right)\right) + \frac{A_4}{\alpha^2}\left(e^{it}\left(\frac{(\text{BesselI}[0,r\zeta]+\text{BesselI}[2,r\zeta])c_1}{2A_4^2} + \frac{(-\text{BesselK}[0,r\zeta]-\text{BesselK}[2,r\zeta])c_2}{2A_4^2}\right) + \frac{1}{r}e^{it}\left(\frac{\text{BesselI}[1,r\zeta]c_1}{\zeta A_4^2} + \frac{\text{BesselK}[1,r\zeta]c_2}{\zeta A_4^2}\right)\right) - \frac{M^2}{\alpha^2}e^{it}\left(\text{BesselI}[0, r\times\zeta]\frac{1}{({A_4}^2\zeta^2)}C_1 - \text{BesselK}[0,r\times\zeta]\frac{1}{({A_4}^2\zeta^2)}c_2 + \frac{\alpha^2\bar{A}}{({A_5}^2\eta^2)}\right) \quad (27)$$

The dimensionless pressure rise is define as

$$\Delta\text{P} = \int_0^1 \frac{\partial \text{p}}{\partial \text{z}}\, dz. \quad (28)$$

$$\Delta \mathrm{P} = -A_1 i e^{it}\left(\frac{\alpha^2 \bar{A}}{\zeta^2 A_4^2} + \frac{\mathrm{BesselI}[0,r\zeta]c_1}{\zeta^2 A4_4^2} - \frac{\mathrm{BesselK}[0,r\zeta]C_2}{\zeta^2 A_4^2}\right) + \frac{A_4}{\alpha^2}\left(e^{it}\left(\frac{(\mathrm{BesselI}[0,r\zeta]+\mathrm{BesselI}[2,r\zeta])C_1}{2A_4^2} + \frac{(-\mathrm{BesselK}[0,r\zeta]-\mathrm{BesselK}[2,r\zeta])C_2}{2A_4^2}\right) + \frac{1}{r}e^{it}\left(\frac{\mathrm{BesselI}[1,r\zeta]C_1}{\zeta A_4^2} + \frac{\mathrm{BesselK}[1,r\zeta]C_2}{\zeta A_4^2}\right)\right) - \frac{M^2}{\alpha^2}e^{it}\left(\mathrm{BesselI}[0, r \times \zeta]\frac{C_1}{({A_4}^2\zeta^2)} - \mathrm{BesselK}[0, r \times \zeta]\frac{C_2}{({A_4}^2\zeta^2)} + \frac{\alpha^2 \bar{A}}{({A_4}^2\zeta^2)}\right). \quad (29)$$

Expression for stream function is given as follows:

$$w(r,t) = \frac{1}{r}\frac{\partial \psi}{\partial r}. \quad (30)$$

3. Results and Discussion

In order to obtain an insight into the physics of the problem, the numerical computations of velocity profile, temperature profile, vorticity, pressure rise, stream lines, skin-friction and Nusselt number are plotted for varied values of magnetic field parameter *M*, kinetic Reynolds number Re_ω, nanoparticle volume fraction ϕ, amplitude of pressure gradient $\bar{A}$, Prandtl number Pr and time *t*.

The axial velocities are studied which varies from inlet to outlet and affect the heat transfer rate in particular region due to development of flow. For one complete pulsation cycle of 360° the instances were taken at each $t = 30^\circ$ to calculate the axial velocity variation at particular volume fraction ϕ. All the captured instances are in total 12 for a complete cycle of 360°. Figures 2(a)-2(d) are ready to study the impact of various values of nanofluid volume fraction on the velocity profile. Each one of these figures depict that the velocity traces a parabolic trajectory with maximum value near the middle of channel and rapidly decreases with rise of nanoparticle volume fraction. It is also illustrated from Figures 2(a)-2(d) that inclusion of nanoparticles provides the increase of density of whole mixture. In figure 2(a), one can observe through margin line that there is a significant and higher disturbance in the velocity profile for base fluid ($\phi = 0$) as compare to the nonzero values of nanoparticle volume fraction. Physically, we can say that by incorporating the nanoparticles (both SWCNTs and MWCNTs) within the engine-oil then the density of whole mixture will increase considerably. Consequently, when density of nanofluid increases then motion of nanofluid become slow as compare to the base fluid (engine-oil) as shown in Figs. 2(a)-2(c).

Figures 3(a)-3(d) shows that the maximum of velocity in a pulsatile flow is found close to walls of the ducts in rapid vibrations, which is called the annular effect, experimentally presented by Richardson et al. [4] and foster analytically by Atabek and Chang [1]. This annular effect increases with the aid of the boom of Womersley number Re_ω. It's also referred to from above figures that addition of nanoparticles diminishes the maximum velocity of the base fluid. It is shown that with increase of Re_w velocity slightly deviate from sinusoidal mean velocity for certain instance of time. With increase of Re_w gives rise to more substantial annular effect and in this way the radial velocity nearby cylinder wall become steeper and friction force increases with increase of Re_w. Inertial component increase in momentum equation with increase of Re_ω. Further it is notice that by increase of Womersley number provides the increase of velocity profile. Since, Womersley number is the ratio of pulsation to the viscous forces and when we increase the Womersley number then viscous forces will reduce. When viscose forces will reduce then motion of the fluid particles become faster and consequently velocity profile will increase gradually (see Fig. 3(a)- 3(d)).

Figure 4(a)-(d) shows that the maximum velocity with increase in the value of Hartmann number M. Yet, close to the upper wall such observation does not hold. Clearly, an increase in the strength of applied magnetic field provides to increase the velocity of nanofluid near the center of the conduit. It's also stated from Figures 4(a)-(d) that adjunct of nanoparticles lessens the maximum velocity of the base fluid. Further it is observed from Fig. 4(a), that engine oil-SWCNT ($\phi = 0.2$) have comparatively low velocity as compare the engine oil ($\phi = 0$). Similar behavior can be observed in Fig. 4(b). It could be comprehended from figures 4(a) and 4(b) that the magnetic field serve as a retardant towards the flow which ends up decrease the flow rate. Furthermore, the magnetic field gives rise to eliminate the annular effect that is considered as a feature of the pulsatile flow. Figure 5(a) and 5(b), demonstrate the variation of Womersley number $\alpha = \sqrt{Re_w}$ to analyze the flow velocity for both base fluid and nanofluid. One can observe in figure 5(a) that for increasing values of Womersley number shows the increasing behavior near the surface of the duct however at the mean position, behavior of velocity profile once rapidly increase for small values of Womersley number and later it is stable for large values of Womersley number. In comparison to Fig. 5(a), it is found in Fig. 5(b) that behavior of velocity profile remains same for engine oil-MWCNT ($\phi = 0.2$) but velocity remnants low.

The variation of vortex profiles attained in the current study has similar results presented by Majdalani [11]. Though, existence of minor variation is virtue of fact that Majdalani [11] design through pulsatile drift passed in a rectangular duct. Fig. 6(a)-6(d) indicates that influence of volume fraction ϕ on the radial profile of vorticity. We note that the magnitude of the vortices is higher when the volume fraction ϕ for nanofluid is small. It should be noted that the vorticity takes negative values for certain phases for different ϕ values indicating the presence of a return flow. In comparison of Fig. 6(a)-6(d), obtained variation in vortex is very high for base fluid ($\phi = 0$) as compare to the non-zero values of nanoparticle volume fraction. Similarly engine-oil based SWCNT ($\phi = 0.2$) have higher disturbance in the vortex as compare to the results obtained for engine-oil based MWCNT ($\phi = 0.2$). The decrease in the flow region ends by the increase in velocity and its miles proven in figures 7(a) and 7(b), where the velocity decreases as nanoparticle volume fraction ϕ increases. In figure 7(a) and 7(b) it is noticed that flow area construct set of envelop for various values of radius and velocity field attained maximum position with respect to increasing values of the radius. Since, internal radius of the cylinder remains less or equal to the radius of external cylinder so domain of the velocity profile restrict from$0 \leq r \leq 1$ so it may be visible that velocity attained maximum within the neighborhood of conduits of flow region that change from 0.7 to 1 and decline in the flow region result in lessen the annular effect. In Fig. 7(b), comparison is made between the engine oil-SWCNT and MWCNT. It found that engine oil-SWCNT have higher velocity profile as compare to the engine oil-MWCNT.

Examination of heat transferal revolves around the study of temperature profile as well as heat transfer rate situated at the wall. Graphs are plotted to study the effects of nanoparticle volume fraction, Hartmann number, pressure gradient amplitude and time on temperature profile. Figures 8(a) shows the variation of dimensionless temperature profile for engine oil-based CNTs for varied volume fraction ϕ. It is spotted that with an increase of nanoparticles enhance the heat transfer profile. Based upon effective thermal conductivity it is further determined that engine-oil based SWCNTs have higher heat transfer rate as compare to the engine-oil based MWCNTs. However base fluid (engine-oil) have low heat transfer rate as compare to the engine-oil based CNTs. Similarly Fig. 8(b) depicts the variation of temperature profile is plotted against Hartmann number M for both SWCTs and MWCNTs. One can observe that fluid temperature rises due to imposition of the transverse magnetic field. Since magnetic field produces the electric current in fluid which produces heat in the fluid, so the magnetic field with radiation

assists the enhancement phenomena. Fig. 8(c) and 8(d) shows the effect of pressure gradient amplitude and time on temperature profile. It is found that increase of pressure gradient amplitude reduce the temperature profile however these results are quite opposite for time t.

Figure 9 and 10 shows the variation of stream line and pressure gradient respectively. In Fig. 9, results are plotted for stream line to analyze the variation of flow behavior for base fluid and engine-oil based CNTs. Similarly pressure gradient is determined for increasing values of nanoparticle volume fraction (both SWCNTs and MWCNTs). In Fig. 10 it is found that, at the mean position of the duct with $t = 180^o$ pressure gradient is maximum but attained the decreasing behavior. However at $t = 0^o$ and $t = 360^o$ pressure gradient is minimum but predicts the increasing behavior with respect to increasing values of nanoparticle volume fraction. It is important to note that in case of engine-oil based SWCNTs have higher pressure gradient as compare to the engine-oil based MWCNTs.

4. Conclusions

We have discussed the MHD pulsatile flow of carbon nanofluid between two concentric ducts. Exact solutions for velocity, pressure and temperature distribution in case of a pulsatile flow for carbon nanofluid is obtained. The influence of magnetic strength on heat transfer has been studied analytically, that is useful for the potential of blood conduct when confronted with magnetic strength. It could be established that the flow of blood and pressure can be managed sufficiently by the application of an external magnetic field. This will guide to abate some arterial diseases. The solution of velocity, pressure and temperature are demonstrated graphically for a wide variety of Reynolds number, volume fractions, and Hartmann numbers. In addition, the outcome confirmed that the temperature might be administer by means of the external magnetic and so the heat transfer could possibly be reduced or improved by acquisitive the acuteness of the magnetic field. Maximum values of velocity decreases through broaden in the CNTs volume fraction. It is also seen that addition of CNTs tremendously increases the temperature of base fluid. Nanofluids are robust coolants than natural base fluids as they are able to get rid of extra warmness than average base fluids. Since, Womersley number is the ratio of pulsation to the viscous forces and when we increase the Womersley number then viscous forces will reduce gradually. And it is found that when viscose forces will reduce then motion of the fluid particles become faster and consequently velocity profile will increase gradually. Significant effects of temperature profile and pressure gradient are analyzed for both SWCNTs

and MWCNTs. In view of effective thermal conductivity it is further determined that engine-oil based SWCNTs have higher heat transfer rate as compare to the engine-oil based MWCNTs.

5. References

[1] H. B. Atabek and C. C. Chang, Oscillatory flow near the entry of circular tube, ZAMP. 12 (1961) 405422.

[2] V. A. Vardanyan, Effect of magnetic field on blood flow, Biofizika, 18(3) (1973) 491-496.

[3] E. G. Richardson, Amplitude of Sound Waves in Resonators, Proceedings of the Physical Society London, 40(27) (1928) 206–220.

[4] E. G. Richardson, E. Tyler, Transverse Velocity Gradient near the Mouths of Pipes in Which an Alternating or Continuous Flow of Air is Established, Proceedings of the Royal Society of London A, 42(1) (1929) 1–15.

[5] J. R. Womersley, Method for the Calculation of Velocity, Rate of Flow and Viscous Drag in Arteries When the Pressure Gradient is Known, Journal of Physiology, 127(3) (1955) 553–563.

[6] S. Uchida, Pulsating Viscous Flow Superposed on the Steady Laminar Motion of Incompressible Fluid in a Circular Pipe, Journal of Applied Mathematics and Physics, 7(5) (1956) 403–422.

[7] A. Yang, L. Chen, Z. Xie, H. Feng, F. Sun, Constructal heat transfer rate maximization for cylindrical pin-fin heat sinks, Applied Thermal Engineering, 108(5) 427-435, (2016).

[8] X. Cui, M.R. Islam, B. Mohan, K.J. Chua, Developing a performance correlation for counter-flow regenerative indirect evaporative heat exchangers with experimental validation, Applied Thermal Engineering, 108(5) 774-784, (2016).

[9] A.E. Dhole, R.B. Yarasu, D.B. Lata, Effect of hydrogen and producer gas as secondary fuels on combustion parameters of a dual fuel diesel engine, Applied Thermal Engineering, 108(5) 764-773 (2016).

[10] Q. Tan, Y. Hu, A study on the combustion and emission performance of diesel engines under different proportions of O2 & N2 & CO2, Applied Thermal Engineering, 108(5) 508-515, (2016).

[11] Muge Elif Orakoglu, Jiankun Liu, Fujun Niu, Experimental and modeling investigation of the thermal conductivity of fiber-reinforced soil subjected to freeze-thaw cycles, Applied Thermal Engineering, 108(5) (2016) 824-832

[12] Marcia H.B. Mantelli, Development of porous media thermosyphon technology for vapor recovering in cross-current cooling towers, Applied Thermal Engineering, 108(5), 398-413 (2016).

[13] D. C. Sanyal and A. Biswas, Pulsatile motion through an axisymmetric artery in presence of magnetic field, Assam University Journal of Science and Technology: Physical Science and Technology, 5(2) (2010) 12-20.

[14] A. Yakhot and L. Grinberg, Phase shift ellipses for pulsating flows, Physics of Fluids, 15(7) (2003) 132-138.

[15] J. Suces, An improved quasi-study approach for transient conjugated forced convection problems, International Journal of Heat and Mass Transfer, 24(10) (1981) 711-1722.

[16] T. W. Latham, Fluid motions in a peristaltic pump, Massachusetts Institute of Technology, (1966) 72-74.

[17] J. Majdalani, Pulsatory channel flows with arbitrary pressure gradients, AIAA.3rd: Theoretical fluid mechanics meeting. (2002) 24-26.

[18] H.L Agrawal, B. Anwaruddin, Peristalic flow of blood in a branch, Ranchi University mathematical journal, 15 (1984) 111-121.

[19] E. E. Tzirtzilakis, A Mathematical Model for Blood Flow in Magnetic Field, Physics of Fluids, 17(7) (2005) 077103-077115.

[20] G. Ramamurthy, B. Shanker, Magneto hydrodynamic Effects on Blood Flow through Porous Channel, Medical and Biological Engineering and Computing, 32(6) (1994) 655-659.

[21] S.U.S. Choi, Enhancing Thermal Conductivity of fluids with Nanoparticles, Developments and Applications of Non-Newtonian Flows, *ASME FED*, 231 (1995) 99-103.

[22] S. U .S. Choi, Nanofluids from vision to reality through research, J. of Heat Transfer, 131 (2009) 1-9.

[23] W. Yu, D.M France, J.L. Routbort, S.U.S. Choi, Review and comparison of nanofluid thermal conductivity and heat transfer enhancements, Heat Transfer Eng., 29 (2008) 432-460.

[24] S.K Das, S.U.S Choi and H.E. Patel, Heat transfer in nanofluids a review, Heat Transfer Eng., 27 (2006) 3-9.

[25] M.S. Liu, M.C.C Lin, I.T. Huang and C.C. Wang, Enhancement of thermal conductivity with carbon nanotube for nanofluids, International Communications in Heat and Mass Transfer, 32 (2005) 1202-1210.

[26] J. Buongiorno, Convective Transport in Nanofluids, J. of Heat Transfer, 128(3) (2005) 240-250.

[27] N.S Akbar, and S. Nadeem, Mixed convective Magnetohydrodynamic peristaltic flow of a Jeffrey nanofluid with Newtonian heating, Zeitschrift fur Naturforschung,68 (2013) 433-441.

[28] A.H Emad and A. Ebaid, New exact solutions for boundary-layer flow of a nanofluid past a stretching sheet, Journal of Computational and Theoretical Nanoscience, 10 (2013) 2591-2594.

[29] S. Ijima, Helical microtubules of graphitic carbon, Nature, 354 (1991) 56–58.

[30] Y. Cheng and O. Zhou, Electron field emission from carbon nanotubes, C.R. Physique, 4 (2003) 1021–1033.

[31] E. V. Timofeeva, J. L. Routbort, D. Singh, Particle shape effects on thermo- physical properties of alumina nanofluids, J. Appl. Phy, 106(1) (2009) 014304-014310.

[32] S. M. Sohel Murshed, C.A. Nietode Castro, M.J.V. Lourenço, M.L.M. Lopes, F.J.V. Santos, A review of boiling and convective heat transfer with nanofluids, Renewable and Sustainable Energy Reviews, 15(5) (2011) 2342–2354.

Table 1: Thermophysical properties of different base fluids and CNTs.

Phase	ρ (Kg/m^3)	K (W/mK)	C (J/kg K)
Engine oil (Base fluid)	884	0.144	1,910
SWCNT(Nanoparticles)	2,600	6,600	425

MWCNT(Nanoparticles)	1,600	3,000	796

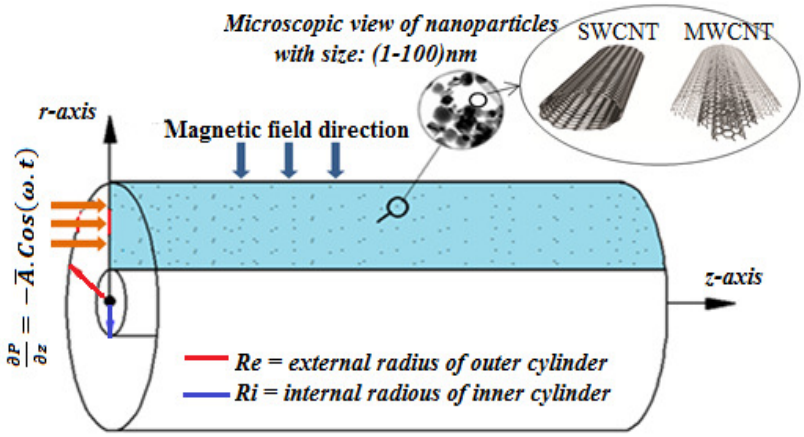

Fig. 1. Geometry of the problem.

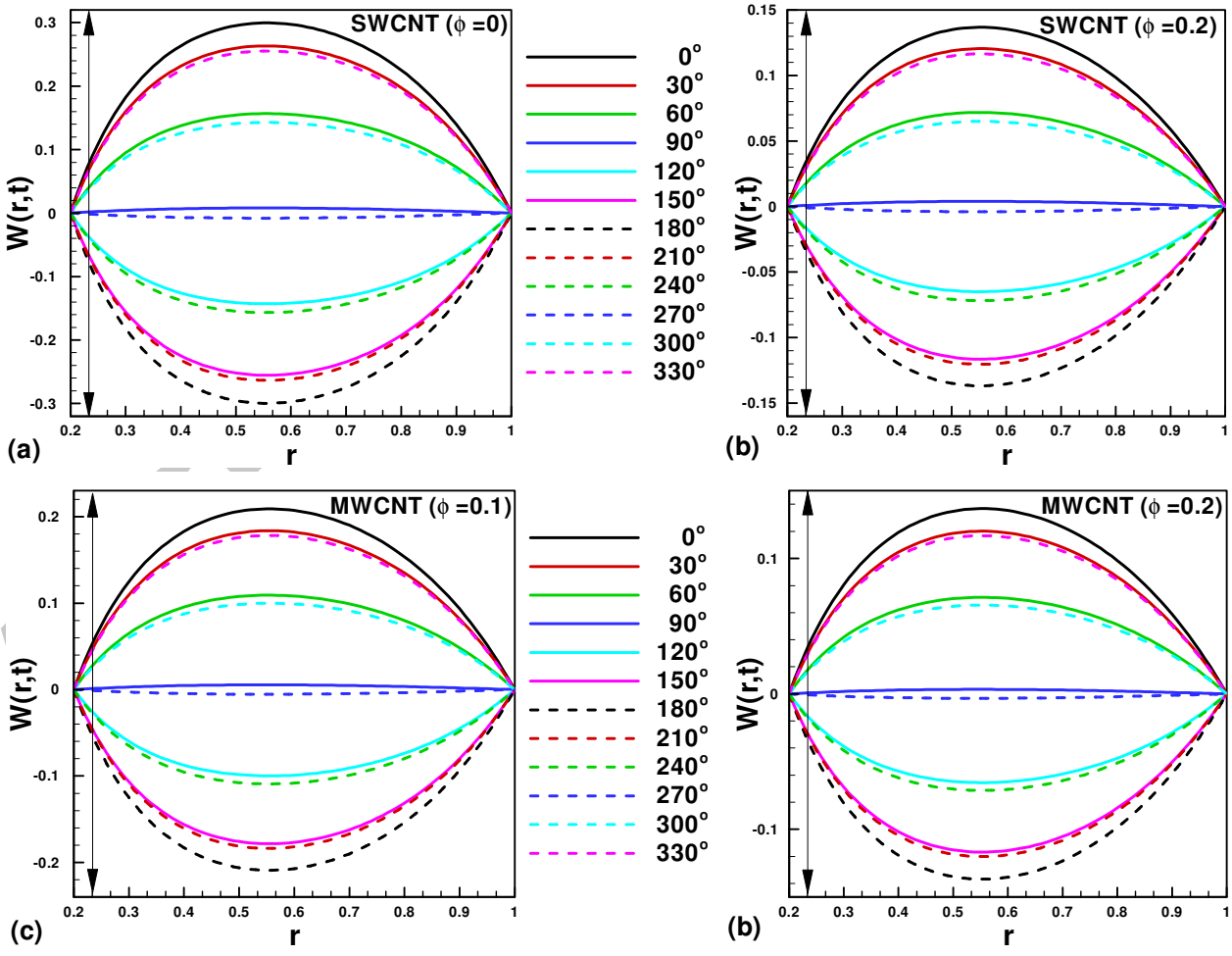

Fig. 2. Variation of velocity profile when $M = 5, Re_\omega = 1$ (a) SWCNT ($\phi = 0$), (b) SWCNT ($\phi = 0.2$), (c) MWCNT ($\phi = 0.1$) (d) MWCNT ($\phi = 0.2$).

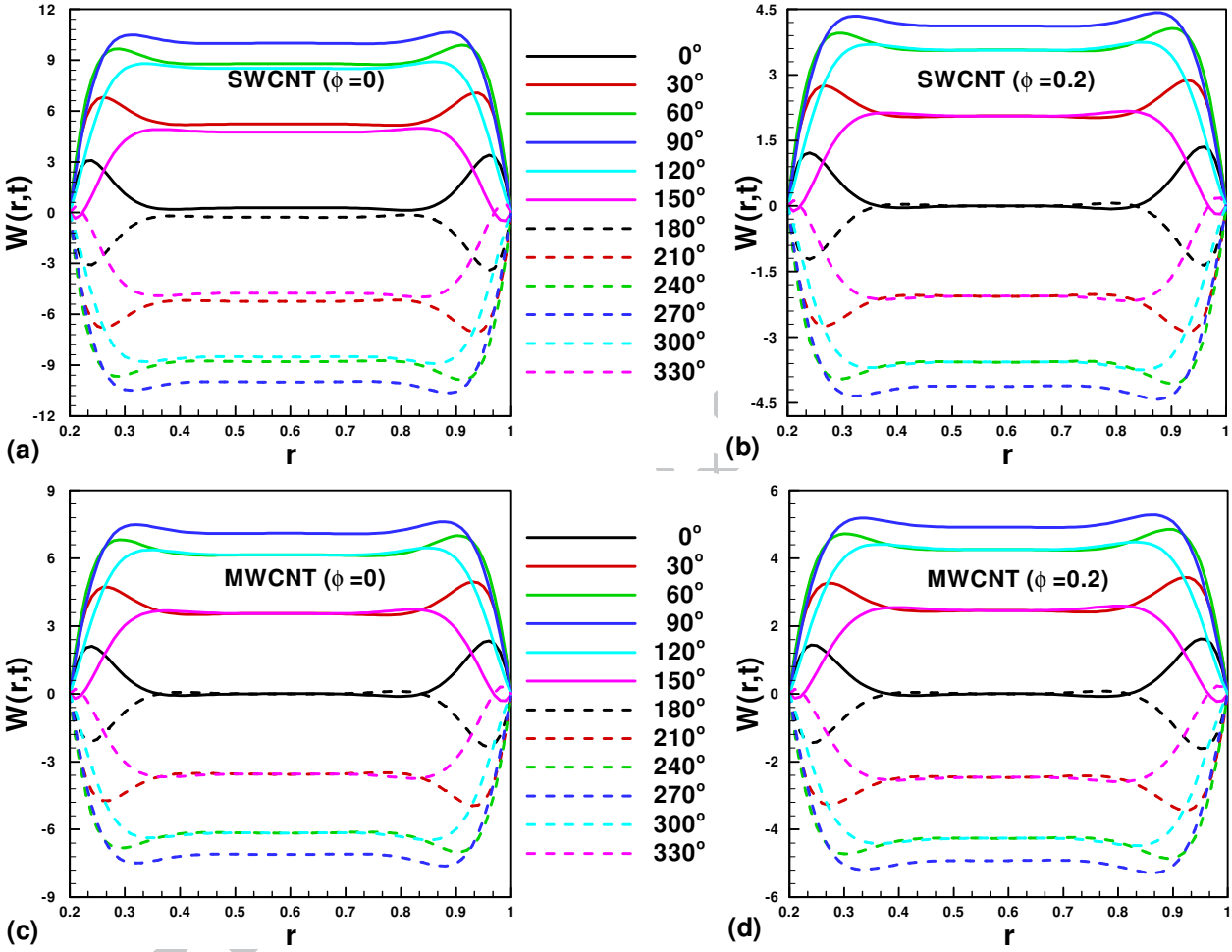

Fig. 3. Variation of velocity profile when $M = 5, Re_\omega = 30$ (a) SWCNT ($\phi = 0$), (b) SWCNT ($\phi = 0.2$), (c) MWCNT ($\phi = 0$) (d) MWCNT ($\phi = 0.2$).

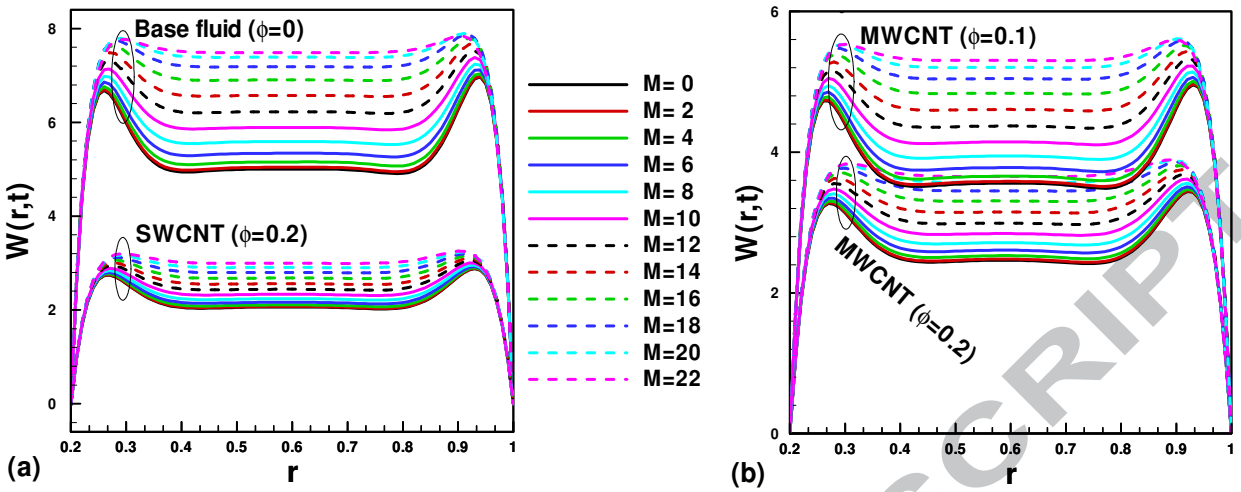

Fig. 4. Variation of velocity profile for various values of M when $t = 30^{\circ}, Re_w = 30$ (a) SWCNT (b) MWCNT.

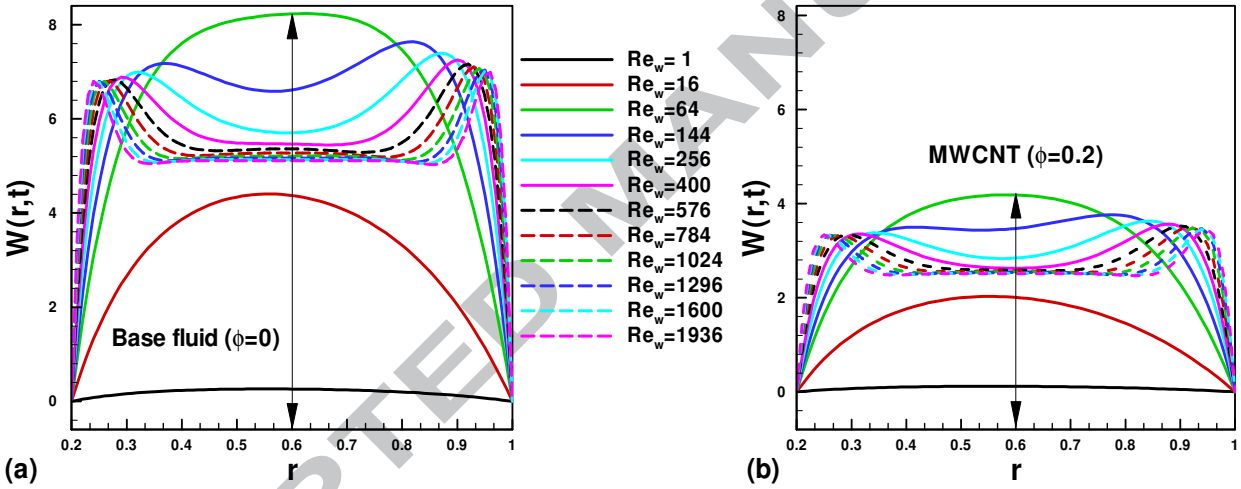

Fig. 5. Variation of velocity profile for various values of Re_w when $t = 30^{\circ}, M = 30$ (a) Base fluid ($\phi = 0$) and (b) MWCNT ($\phi = 0.2$).

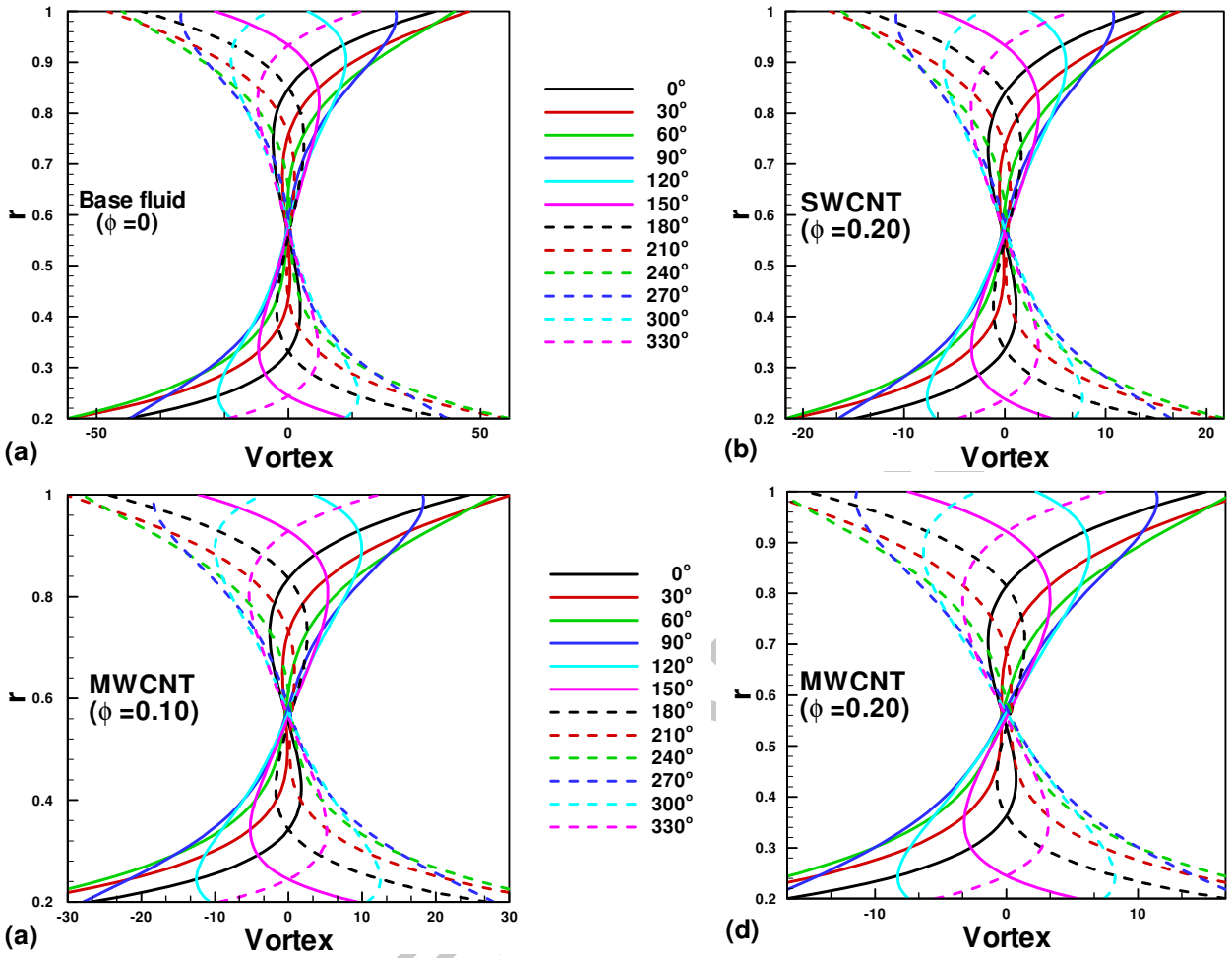

Fig. 6. Variation of vortex profile t for (a) Pure fluid $(\phi = 0)$, (b) SWCNT $(\phi = 0.2)$, (c) MWCNT $(\phi = 0.1)$ (d) MWCNT $(\phi = 0.2)$ when $Re_\omega = 10, M = 5$.

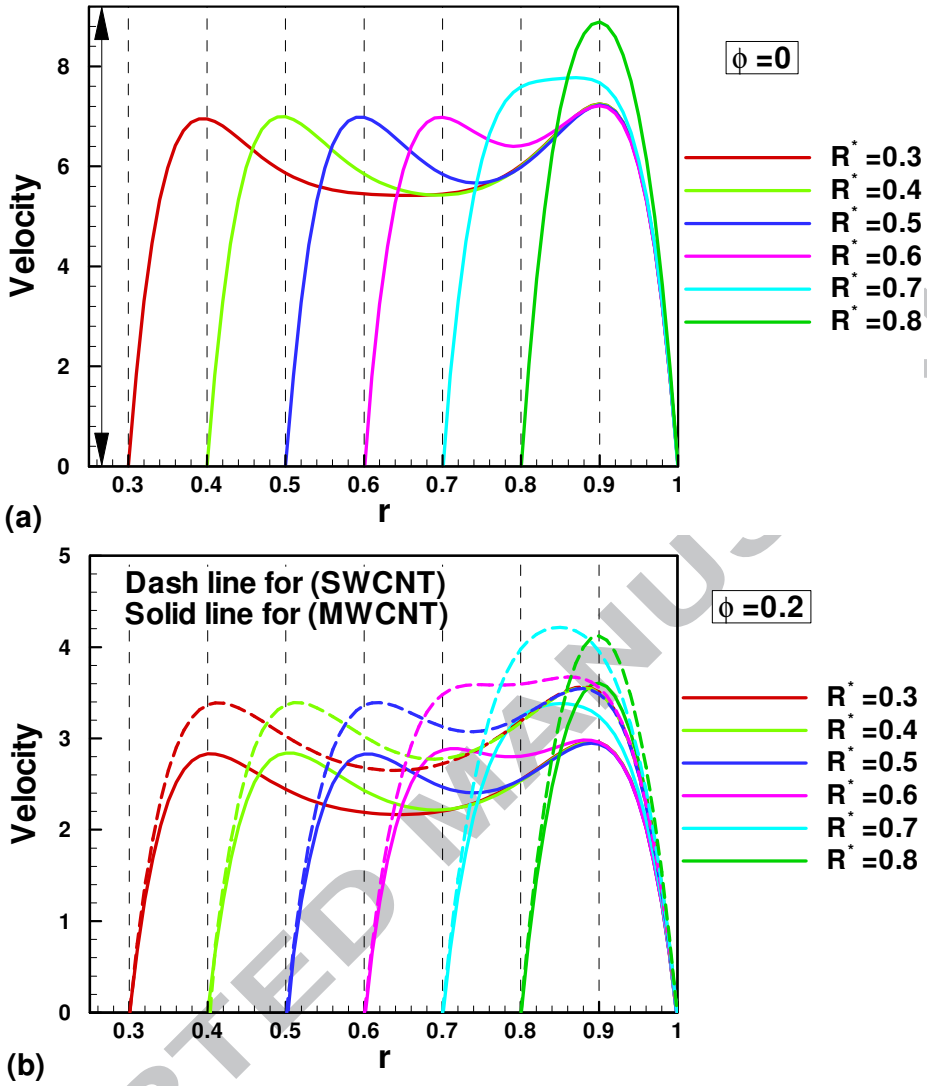

Fig. 7. Variation of velocity profile for various values of R^* (a) Pure fluid $(\phi = 0)$, (b) SWCNT and MWCNT $(\phi = 0.2)$.

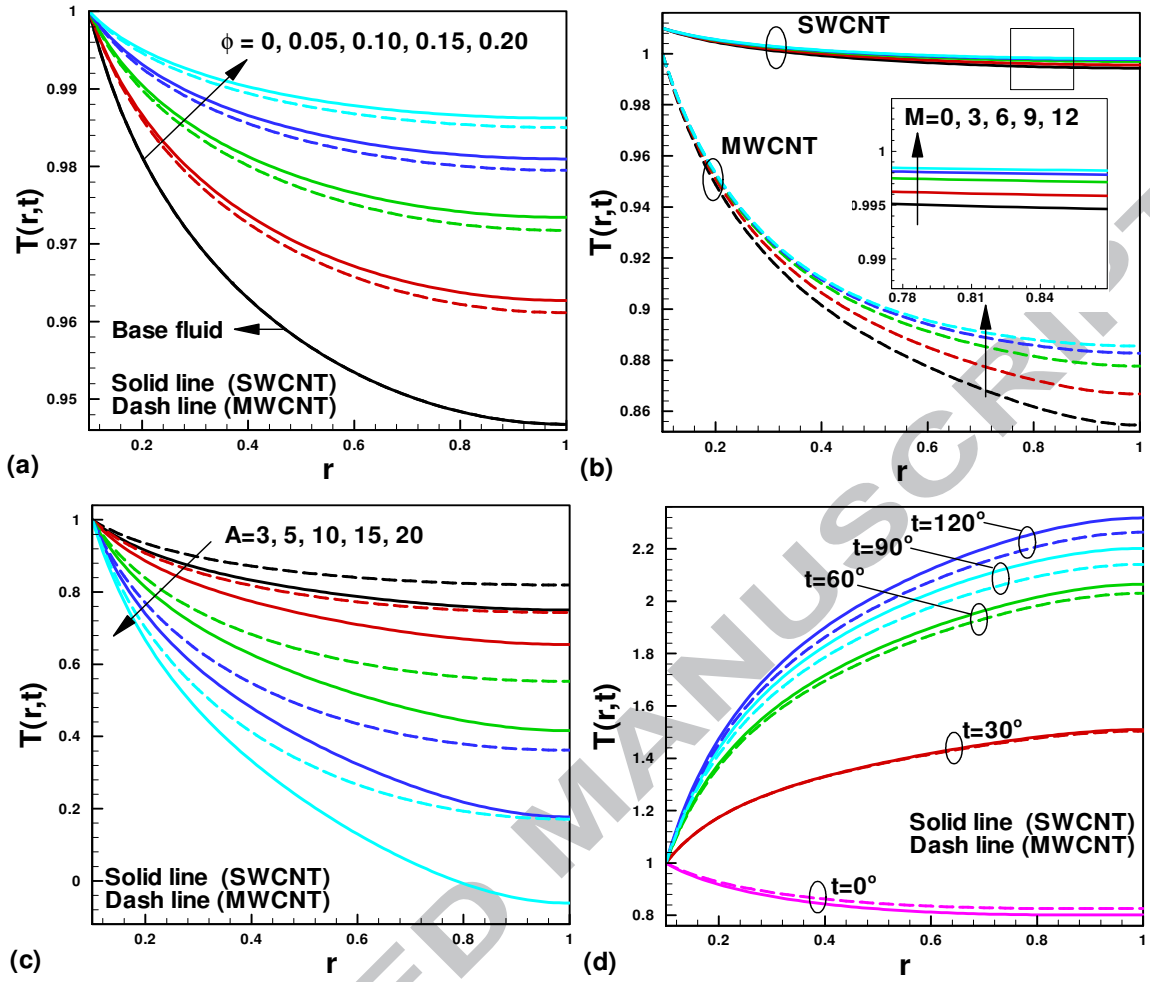

Fig.8. Variation of temperature profile for various values of (a) nanoparticles ϕ, (b) Hartmann number M, (c) amplitude of pressure gradient $\overline{A}$ and (d) time t.

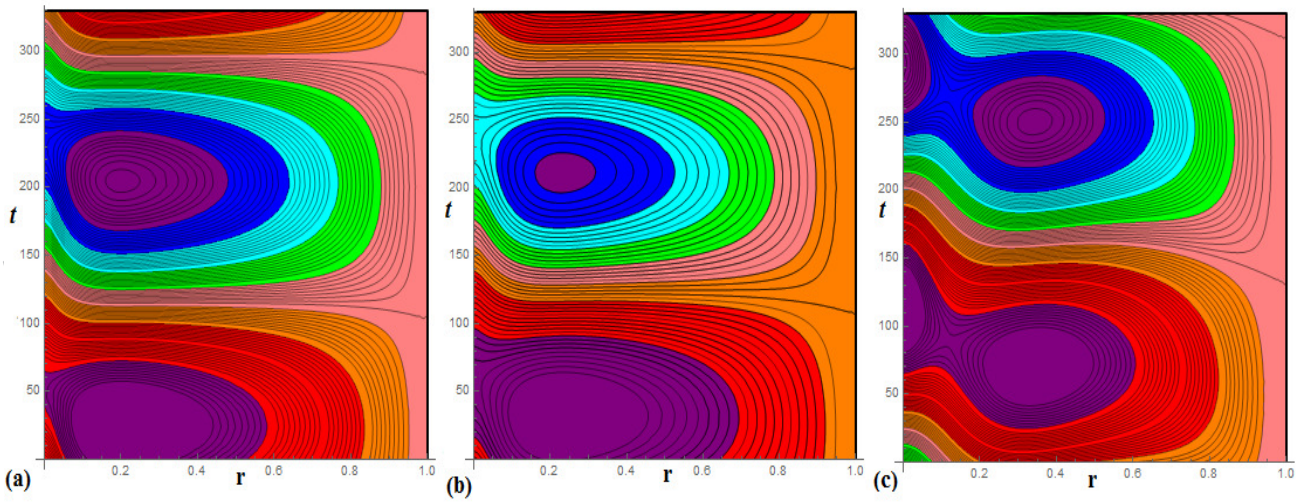

Fig. 9. Streamlines for engine oil- based CNTs for **(a)** base fluid ($\phi = 0$) **(b)** SWCNT ($\phi = 0.2$) and **(c)** MWCNT ($\phi = 0.2$).

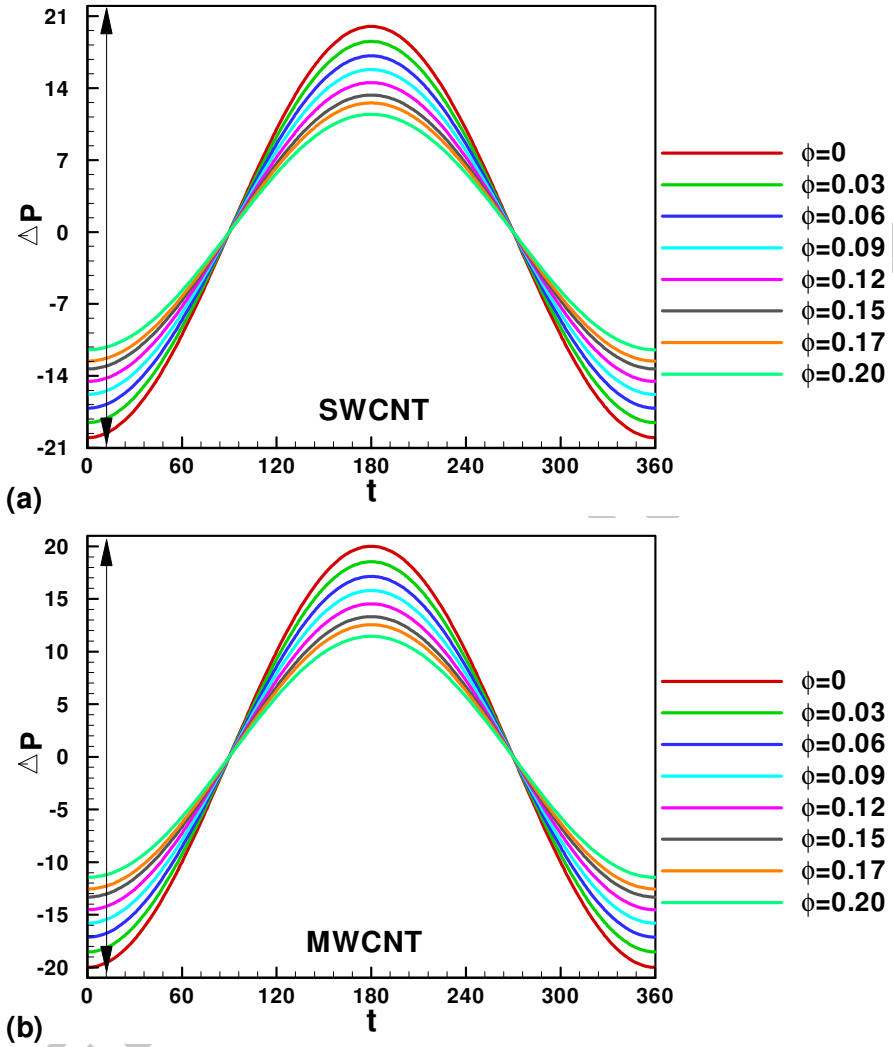

Fig. 10: Pressure gradient for (a) SWCNT and (b) MWCNT, when $\bar{A} = 20, M = 10, \alpha = 10$ and $R^* = 0.2$.